

Sub-10-femtosecond active synchronization of two passively mode-locked Ti:sapphire oscillators

Long-Sheng Ma,^{*} Robert K. Shelton, Henry C. Kapteyn, Margaret M. Murnane, and Jun Ye[†]
JILA, National Institute of Standards and Technology and University of Colorado, Boulder, Colorado 80309-0440
 (Received 30 November 2000; published 10 July 2001)

Two independent mode-locked femtosecond lasers are synchronized to an unprecedented precision. The rms timing jitter between the lasers is 4.3 fs, observed within a 160-Hz bandwidth over minutes. Multistage phase-locked loops help to preserve this ultrahigh timing resolution throughout the entire delay range between pulses (10 ns). We also demonstrate that the same level of synchronization can be achieved with two lasers at different repetition frequencies.

DOI: 10.1103/PhysRevA.64.021802

PACS number(s): 42.65.Re, 06.60.Jn, 42.62.Eh

The use of ultrashort light pulses to study coherent interactions in atomic and molecular systems has advanced rapidly in recent years. One exciting area of current research is in “coherent control,” where light pulses that have been precisely shaped in amplitude and phase can selectively “drive” [1] a chemical reaction [2], molecular vibration [3], or other process such as nonlinear-optical conversion of light into the extreme ultraviolet region [4].

However, current experimental techniques are still very limited in their ability to coherently control the evolution of quantum systems. In the most general case, coherent control techniques require phase-coherent, femtosecond, temporally shaped pulses over a large region of the spectrum, to be able to access all possible intermediate states in a multistep quantum “pathway” to achieve the desired outcome [5]. Broadest-bandwidth ultrashort-pulse lasers generate only a fractional bandwidth on order of 30% of their carrier frequency. Nonlinear-optical techniques such as white-light continuum generation [6] and parametric amplification [7] can be used to generate coherent light over a broad spectrum. However, these techniques often suffer from poor efficiency. Furthermore, often the quantum transitions for a process of interest for coherent control are concentrated in a few disparate regions of the spectrum. It would thus be desirable to be able to take two separate laser systems, generating light with distinct optical properties, and precisely synchronize the output of both lasers, essentially generating a single, composite coherent light field. This ability to precisely synchronize separate, pulsed laser sources is an important step toward the ultimate, “arbitrary light wave-form generator.” It is also important for a number of other technologies, such as mid-infrared light generation through difference frequency mixing [8], for experiments requiring synchronized laser light and x rays or electron beams from synchrotrons [9], and also for the synthesis of light pulses with shorter duration than is obtainable from any single individual laser [10].

Synchronization and phase locking of separate femtosecond lasers will also have a strong impact in precision frequency metrology based on optical frequency combs [11,12], providing the capability of a wide-bandwidth phase-coherent

frequency network covering various spectral regions. Frequency-domain control of femtosecond combs not only provides an effective means to transfer the stability of a cw optical oscillator to the entire comb [13], but also has a strong impact on the time-domain evolution of carrier-envelope phase [14]. The frequency mode spacing of the femtosecond comb is equal to the inverse of the cavity round trip time of the laser; hence reduction of the phase noise of the repetition rate spectrum directly improves the control of the timing jitter.

To date, previous work in synchronizing separate mode-locked Ti:sapphire lasers demonstrated a timing jitter of at best a few hundred femtoseconds [15,16]. Since it is now routine to generate pulses with duration <20 fs, improved techniques would make it possible to take full advantage of this time resolution for immediate application in various fields.

In this Rapid Communication, we demonstrate robust synchronization of pulse trains from two separate femtosecond lasers, with a timing jitter of <5 fs, at a bandwidth of 160 Hz, observed over several minutes. The two independent mode-locked Ti:sapphire lasers [17] operate at 780 and 820 nm, respectively, with ~ 100 -MHz repetition rates. The bandwidth of both lasers corresponds to a transform limit of <20 fs mode-locked pulses. Our synchronization scheme, shown in Fig. 1, employs two high-speed photodiodes to detect the two pulse trains. These signals are then input to four phase locked loops (PLL's) working at different timing resolutions. Using the first PLL, we synchronize the repetition rate of

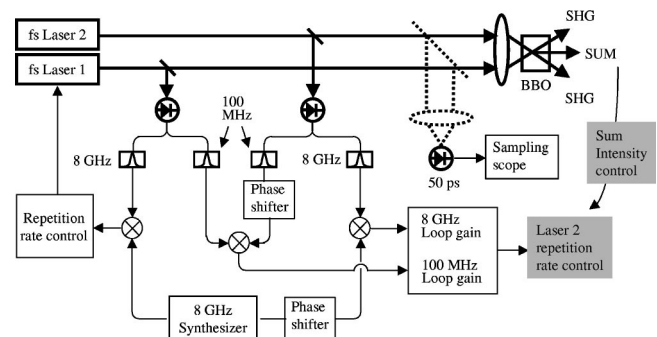


FIG. 1. Experimental setup for timing synchronization of two femtosecond lasers. The four phase-locked loops for synchronization are shown, along with the signal analysis scheme.

^{*}Permanent address: East China Normal University, Shanghai, China.

[†]Corresponding author. Email address: ye@jila.colorado.edu

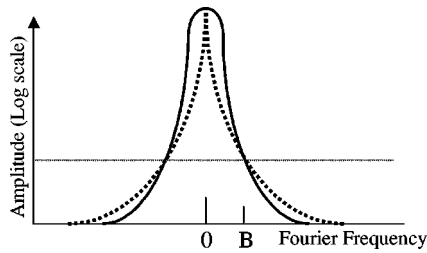


FIG. 2. Phase noise spectra of the microwave reference signal (dotted curve) and the detected laser repetition signal (solid curve). At frequencies higher than B , the laser has intrinsically less noise than the reference.

laser 1 to a stable rf source, with an in-loop error signal indicating an rms timing jitter less than 10 fs over a bandwidth of 10 kHz. Laser 2 is synchronized directly to laser 1 using a second PLL, which compares and locks the fundamental frequencies of the two lasers at 100 MHz. The phase shift between the two 100-MHz signals can be used to control the timing offset between two pulse trains. The third PLL compares the phase of the 80th harmonic of the two repetition frequencies; i.e., at 8 GHz. The third loop is activated, and replaces the second one when the two pulse trains are nearly overlapped. This represents an electronic realization of a “differential micrometer”—the 100-MHz loop provides the full dynamic range of timing offset between two pulse trains, while the 8-GHz loop produces an enhanced phase stability of the repetition frequency. To further minimize jitter, the intensity of the sum frequency signal from the two pulse trains overlapped in space and time is directly used as a control error signal for a fourth loop. This fourth loop can be usefully activated only when the 8-GHz PLL is working effectively, and most timing jitter noise has already been eliminated. All four loops actuate fast (>50 -kHz bandwidth) piezotransducers (PZT) mounted to the laser end mirrors.

The motivation for using a high harmonic for phase locking the repetition rate is to obtain an enhanced signal-to-noise (S/N) ratio. In Fig. 2 the solid curve represents the detected phase noise power spectrum of the laser repetition signal, while the dotted curve indicates the microwave reference to which the repetition signal is locked. Experimental data show that the laser repetition signal has less fast phase noise than the rf reference beyond frequency B (around 10 kHz) indicated in Fig. 2. Therefore, the servo loop bandwidth should be limited to below B , provided that the noise floor of the repetition detection is a few dB below the dashed line. If the detection S/N ratio is not sufficiently high, then the servo bandwidth will be further limited. Detection at a high harmonic can help to avoid this problem. The high-speed photodiodes used in this experiment suffer a loss of S/N ratio of only 3 dB when the repetition signal is detected at the 80th harmonic, compared with the S/N ratio at the fundamental. When analyzed at the fundamental while stabilized at the 80th harmonic, the repetition signal thus enjoys an effective increase in the S/N ratio of 16 dB.

Figure 3 shows the effective use of combined PLL’s for the control of the timing offset between two pulse trains. The second pulse train is scanned relative to the first via a phase shift inside the 100 MHz loop, showing the full range scan-

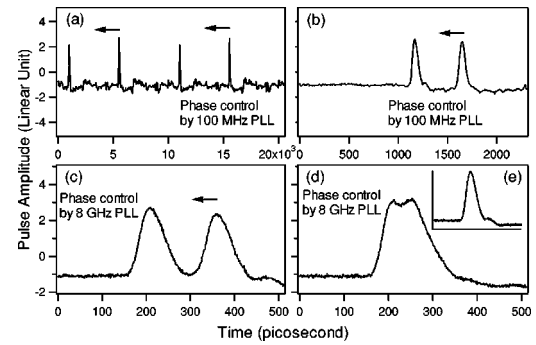


FIG. 3. Control of the relative timing offset between the two independent pulse trains using the combined phase locked loops. (a) Two independent pulse trains incident on a same photodiode, with a repetition period of 10 ns. (b) Expanded time axis, 100 MHz PLL control. (c) The time scale is further expanded, 8 GHz PLL control. (d) Two pulses nearly overlapped via adjustment of the 8-GHz phase shifter. (e) Two pulses maximally overlapped.

ning capability in Figs. 3(a) and 3(b). Once the two pulses are within 200 ps of each other, we gradually reduce the gain of the 100-MHz PLL and increase the gain of the 8-GHz loop, leading to a smooth transition between the two loops and a small jump of the timing offset by at most 62.5 ps (one-half of one 8-GHz cycle). Tuning of the timing offset can then be continued with the 8-GHz loop, as shown in Figs. 3(c) and 3(d) with an expanded time axis. The two pulses are maximally overlapped in Fig. 3(e).

To characterize our system further, we focus the two pulse trains so that they cross in a 500- μm -thick, room temperature, BBO crystal for nonlinear frequency generation (type I). Figure 4(a) shows the generated second-harmonic light from two pulse trains after the crystal. When the two pulses are overlapped in space and time, sum-frequency generation is enabled, as shown with the bright spot in the center of Fig. 4(b). We can thus use the intensity of the sum-frequency generation as a diagnostic tool to study our system performance. Figure 4(c) shows a cross-correlation measurement

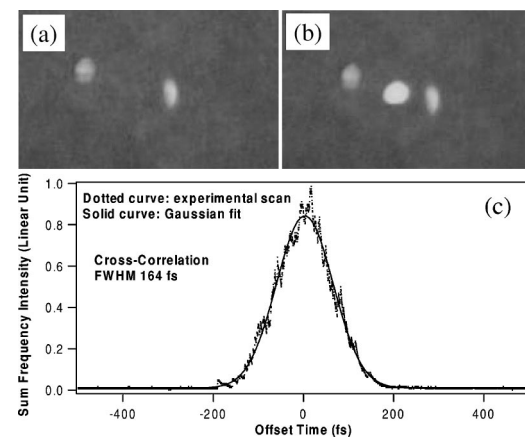


FIG. 4. (a) Second-harmonic generation from two spatially crossed pulse trains in a BBO crystal. (b) Sum generation is enabled when the two pulses are synchronized and overlapped. (c) Cross-correlation measurement via the electronic scan of the relative phase.

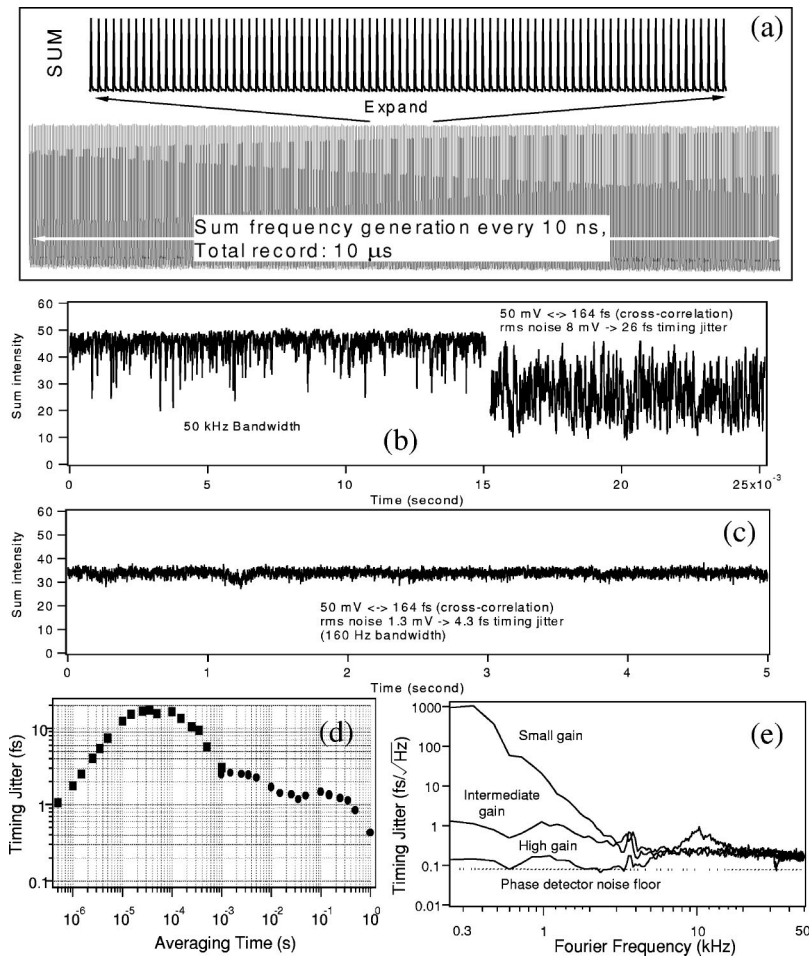


FIG. 5. Timing jitter noise analysis. (a) A 10- μ s direct digitization record of the sum-frequency generation. Also shown is the time-expanded trace. (b) Sum-frequency generation observed with a 50-kHz bandwidth. The left trace shows two pulses optimally overlapped, and the right trace shows two pulses offset by a half-width. (c) Sum signal observed under a 160-Hz bandwidth, showing a rms timing jitter noise of 4.3 fs. (d) Allan variation of the timing stability, showing that the maximum jitter occurs around 10–100 μ s. (e) Fourier frequency spectrum of the error signal from the 8-GHz phase-locked loop.

between the two pulses, carried out by a simple electronic sweep of the relative phase inside the 8-GHz PLL. The Gaussian full width at half maximum (FWHM) of the cross-correlation peak is 164 fs. This compares well with a theoretical estimate of 160 fs, based on the measured pulse widths of 82 and 138 fs for the individual lasers. (Because no extra-cavity dispersion compensation is used, the 20-fs laser pulses are broadened due to dispersion.) Compared to a mechanical scanning system, this electronic tuning method offers a vastly superior performance in terms of the repeatability, reliability, and speed for setting the time offset, with no noticeable hysteresis when we switch back and forth between two preselected phase values.

The intensity fluctuations in the generated sum-frequency light are proportional to the timing jitter, particularly when the two pulses are offset in time by $\sim 1/2$ the pulse width. At short time scales, the intensity fluctuation of the sum frequency light can be studied by simply recording the pulse-to-pulse variation. Using a nanosecond-speed photodiode and nanosecond sampling rates, we have directly digitized the sum frequency pulse train over a period of 10 μ s. The recorded data are shown in Fig. 5(a), along with the expanded trace, when the relative timing offset between the two original pulse trains is near zero. The pulse-to-pulse variation of the sum-frequency signal is basically the same as that of the original laser pulses, below a level of 0.4%. Since the bandwidth of our servo loop does not quite reach the

10- μ s time scale, this superior timing stability is attributed entirely to the free-running lasers due to the lack of environmental disturbance on such short-time scales. At longer time scales, the intensity fluctuation in the sum-frequency signal can be explored with an appropriate low-pass filter to avoid sampling noise. A 50-kHz low-pass filter is sufficient to suppress the discrete nature of the pulse train, and permit the study of intensity fluctuations on a cw basis. In Fig. 5(b), the left trace shows the sum-frequency intensity fluctuation when the two pulse trains are maximally overlapped, while the right trace is recorded when the two pulses are offset in time by $\sim 1/2$ the pulse width. For the right trace, the sum-frequency signal is monitored near the middle point of the cross-correlation peak shown in Fig. 4(c). Therefore, the intensity fluctuations can be translated linearly into timing jitter noise using the calibrated slope of the correlation peak. For a maximum intensity of the sum-frequency light at 50 units, and the FWHM of the cross-correlation peak at 164 fs, we can conservatively estimate the conversion scale of the slope at 3.3 fs/unit. The rms timing noise from the right trace is thus determined to be ~ 26 fs at a 50-kHz bandwidth. At higher bandwidths, the jitter does not increase. If we use a bandwidth of 160 Hz (equivalent to 1-ms averaging time) the resultant intensity fluctuations of the summing light shown in Fig. 5(c) indicates a rms timing jitter noise of 4.3 fs. We have recorded such a stable performance over periods extending over tens of minutes. The advantage of the high harmonic

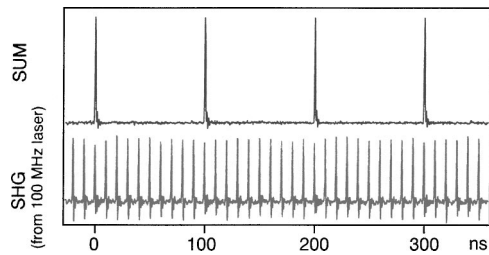


FIG. 6. Sum-frequency generation from two synchronized femtosecond lasers that have different repetition rates, one at 90 MHz and the other at 100 MHz. The second harmonic signal from the 100-MHz laser is also shown.

PLL over the 100-MHz loop is particularly clear from the recorded sum frequency intensity, exhibiting fluctuations more than 20 times larger when under the 100-MHz control. The synchronization lock can be maintained for durations of several hours.

It is interesting to explore further the issue of the timing jitter noise vs its characteristic time scales (or, equivalently, its frequency spectrum). Allan variance analysis [18] is a powerful technique developed to separate and isolate processes based on their time scales. The approach uses a first-difference calculation, and compares adjacent measurements segmented within certain time windows. This is useful to identify time scales at which fluctuations are the largest. From the time record of the timing jitter noise shown in Figs. 5(b) and 5(c), we calculate the Allan variance of the timing jitter. The result is shown in Fig. 5(d). The “square” data points correspond to the fast time record [the right trace in Fig. 5(b)] while the “circular” data points correspond to the longer record [shown in Fig. 5(c)]. It is clear from this analysis that the dominant timing jitter noise occurs within 10–100 μ s, a region where the gain of the PLL loop is rolling off from the low-frequency end while the external perturbations to the laser are increasing from the high-frequency end. However, it is satisfying to find that the timing jitter noise never exceeds 20 fs at any time scale.

These results can be confirmed through the equivalent analysis of the error signal within the PLL servo loop [19]. Figure 5(e) shows the Fourier spectrum analysis of the error

signal at different gain settings. When the loop is operated stably with a high gain, within a frequency range from dc to 5 kHz, the error signal is very close to the limit (≤ 0.1 fs/ $\sqrt{\text{Hz}}$) set by the intrinsic noise floor of the 8-GHz phase comparator used in the PLL. A small servo bump appears near 10 kHz, and rolls off to a flat noise floor near 0.14 fs/ $\sqrt{\text{Hz}}$. Integrating the noise density over the interested spectral range (from dc to 50 kHz) would yield a rms timing jitter of ~ 30 fs, slightly larger than the direct time-domain data.

This synchronization system is flexible in that it can lock two independent lasers working at different repetition rates. The 81st harmonic of the repetition rate of laser 1, still operating at 100 MHz, is compared to the 90th harmonic of laser 2, now running at 90 MHz. The two pulse trains will then collide in the time domain every 100 ns, leading to a sum-frequency pulse train at a 10-MHz repetition rate. The result is shown in Fig. 6, where the top trace reflects the summing frequency generation and the bottom trace is the second-harmonic generation of the 100-MHz laser. Note the slight decrease in the second-harmonic intensity when sum-frequency generation occurs with two pulses overlapped. This approach can be generalized to produce sum- and difference-frequency generations with arbitrary repetition rates, yet perfectly synchronized to the master frequency.

In summary, we have synchronized two independent femtosecond lasers to an unprecedented precision. The remaining rms timing jitter between the lasers is 4.3 fs, observed within a 160-Hz bandwidth. This ultrahigh timing resolution is available through the entire dynamic range of pulse repetition period (10 ns). Such synchronization can be achieved with two lasers at different repetition frequencies. The synchronization work has proved essential for the first realization of an optical carrier phase lock between independent femtosecond lasers [20], paving the way for eventual pulse synthesis from different lasers.

We are indebted to J. L. Hall for his strong support of this work. We also thank S. T. Cundiff for useful discussions, and D. Anderson and the KMLabs for the loan of pump lasers. The work at JILA was supported by NIST, NASA, NSF, and the Research Corporation.

[1] R. Judson and H. Rabitz, *Phys. Rev. Lett.* **68**, 1500 (1992).
 [2] A. Assion *et al.*, *Science* **282**, 919 (1998).
 [3] A. M. Weiner *et al.*, *Science* **247**, 1317 (1990).
 [4] R. Bartels *et al.*, *Nature (London)* **406**, 164 (2000).
 [5] H. Rabitz, *Adv. Chem. Phys.* **101**, 315 (1997); T. H. Yoon *et al.*, *Phys. Rev. A* **63**, 011402(R) (2001).
 [6] R. R. Alfano, *The Supercontinuum Laser Source* (Springer-Verlag, New York, 1989).
 [7] P. Corkum *et al.*, *Opt. Lett.* **19**, 1973 (1994).
 [8] R. A. Kaindl *et al.*, *J. Opt. Soc. Am. B* **17**, 2086 (2000).
 [9] R. W. Schoenlein *et al.*, *Science* **274**, 236 (1996).

[10] J. P. Zhou *et al.*, *Opt. Lett.* **19**, 1149 (1994).
 [11] Th. Udem *et al.*, *Phys. Rev. Lett.* **82**, 3568 (1999).
 [12] S. A. Diddams *et al.*, *Phys. Rev. Lett.* **84**, 5102 (2000).
 [13] J. Ye *et al.*, *Opt. Lett.* **25**, 1675 (2000).
 [14] D. J. Jones *et al.*, *Science* **288**, 635 (2000).
 [15] D. E. Spence *et al.*, *Opt. Lett.* **19**, 481 (1994).
 [16] S. A. Crooker *et al.*, *Rev. Sci. Instrum.* **67**, 2068 (1996).
 [17] M. T. Asaki *et al.*, *Opt. Lett.* **18**, 977 (1993).
 [18] D. W. Allan, *Proc. IEEE* **54**, 221 (1966).
 [19] H. Tsuchida, *Opt. Lett.* **24**, 1641 (1999).
 [20] R. K. Shelton *et al.* (unpublished).